NANO LETTERS

Letter

pubs.acs.org/NanoLett

Doping and Quantum Confinement Effects in Single Si Nanocrystals Observed by Scanning Tunneling Spectroscopy

O. Wolf,[†] M. Dasog,[‡] Z. Yang,[‡] I. Balberg,[†] J. G. C. Veinot,*[,‡,§] and O. Millo*[,†]

[†]Racah Institute of Physics and the Center for Nanoscience and Nanotechnology, The Hebrew University of Jerusalem, Jerusalem 91904, Israel

[‡]Department of Chemistry, University of Alberta, Edmonton, Alberta T6G 2G2, Canada

[§]NRC-National Institute for Nanotechnology, Edmonton, Alberta, T6G 2M9, Canada

Supporting Information

ABSTRACT: We have applied scanning tunneling spectroscopy in studies of the electronic level structure of surface-functionalized colloidal Si nanocrystals (Si-NCs) as a function of their size for various capping ligands. The energy gaps extracted from the tunneling spectra increase with decreasing NC size, manifesting the effect of quantum confinement. This is consistent with the blueshift revealed by photoluminescence (PL) from dodecene functionalized Si-NCs. The tunneling spectra measured on NCs functionalized with NH_4Br or allylamine show band-edge shifts toward higher energies, akin to p-type doping. This behavior can be accounted for by the combined contributions of the ligands' dipole moments and charge transfer between a Si-NC and its surface groups. Concomitantly, size-independent PL spectra, which cannot be associated with NC band gap variations, were observed for the latter Si-NCs.

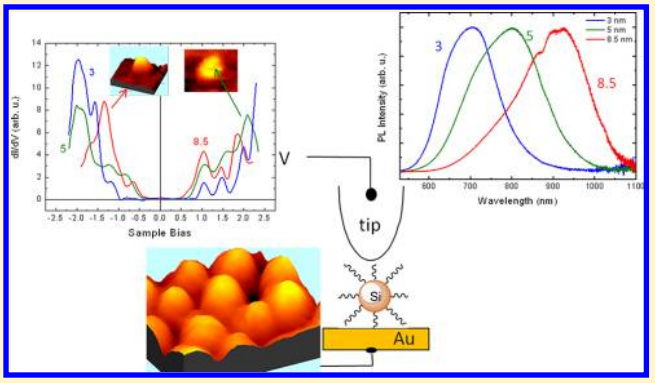

KEYWORDS: *Silicon nanocrystals, quantum confinement, scanning-tunneling-spectroscopy, surface-doping, photoluminescence*

Colloidal silicon nanocrystals (Si-NCs) are attracting considerable interest in recent years because of their intriguing electronic, optical, and chemical properties. Their anticipated biocompatibility[1] makes them particularly appealing for applications in consumer optoelectronic,[2−4] photovoltaic devices,[5,6] and as fluorescent labels for biological sensing.[7,8] In addition, the natural abundance of Si and its prevalence in microelectronics may facilitate their adoption into optoelectronic applications. An important step toward this end is found in recent advancements in synthesis of size and shape-controlled Si-NCs, which allow exquisite control over their optical properties (i.e., absorption and photoluminescence (PL) spectra). Integration of semiconductor NCs into devices often requires tuning their electronic level positions relative to other components. This can be done by surface functionalization with appropriate ligands[9] (that could be considered surface-doping) or by "bulk" doping with impurity atoms, as demonstrated recently for direct band gap InAs[10] and CdSe[11] NCs. The influence of these parameters has yet to be investigated for indirect band gap Si-NCs. One of the goals of the present work is to demonstrate controlled manipulation of the quantized energy levels in Si-NCs via surface ligand tailoring. In a broader perspective, finding and, more importantly, understanding various routes for surface functionalization of Si-NCs is essential given the established reactivity of hydride-terminated Si-NCs.

An important aspect still lacking in studies of colloidal Si-NCs is the characterization of their electronic properties, including the single-particle (as opposed to the excitonic) band gap and the charging (addition) energies, at the single NC level. These parameters were measured using differential pulse voltammetry by Ding et al.,[12] although not for single NCs. Scanning tunneling microscopy and spectroscopy (STM and STS) have proven to be among the most effective tools for the study of electronic properties of single colloidal semiconductor NCs (mainly from the III−V and II−VI groups), both isolated or within arrays,[13−17] particularly when combined with optical measurements.[18] In studies of Si-NCs, this combination becomes even more essential in context of the longstanding controversy regarding the association of optical spectroscopy results, in particular PL, with Si-NC level-structure.[19] This controversy stems from two difficulties. First, for optical experiments in general one cannot determine a priori where carrier excitation (and/or recombination) takes place. Second, where Si species are involved, some oxidation is usually present and thus optical observations have been attributed, in many works, to various oxide phases and defects within them or

Received: February 13, 2013
Revised: April 23, 2013

dx.doi.org/10.1021/nl400570p | *Nano Lett.* XXXX, XXX, XXX−XXX

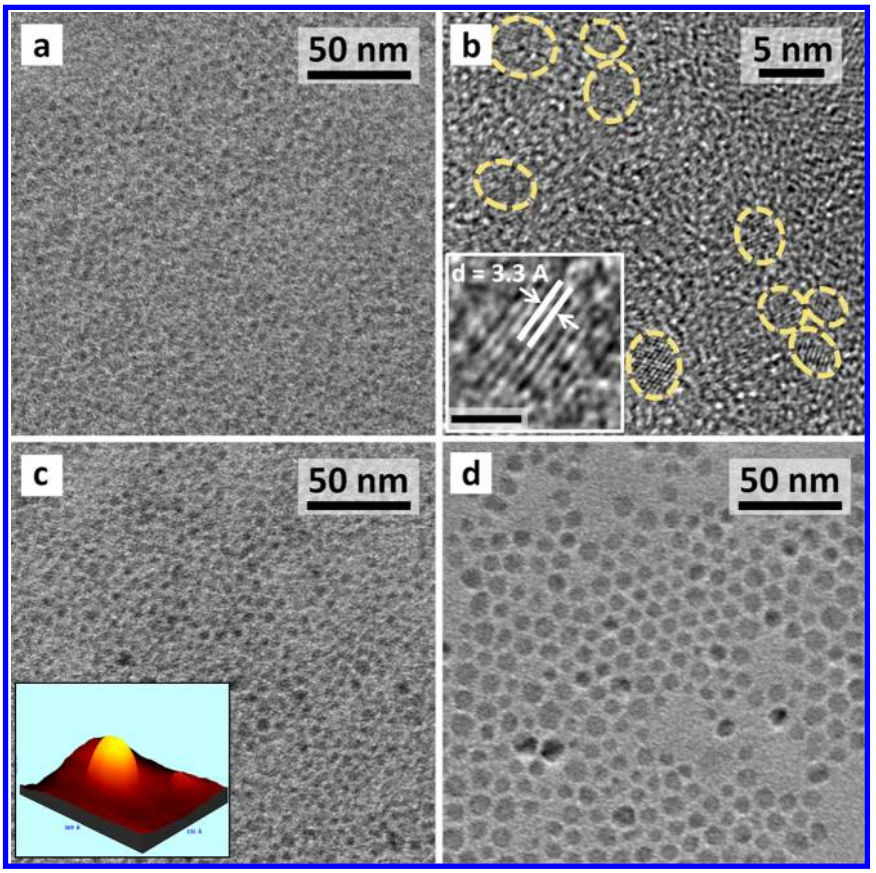

Figure 1. Bright-field TEM images of ensembles of dodecyl surface terminated silicon nanocrystals with several average diameters: (a,b) 3.1, (c) 5.1, and (d) 8.3 nm (see Supporting Information Figure S3 for the size distribution). Inset of b: magnified HRTEM image of a single 3 nm silicon nanocrystal (scale bar = 2 nm); the crystallinity of the NCs is verified also by the XRD data presented in Supporting Information Figure S4(c). Inset of c: STM topographic image of a single 3 nm diameter Si NC.

defects at the Si−oxide interface. In particular, it has been found that in Si-NC systems the band gap widening, commonly associated with quantum confinement (QC), may actually be concealed by the aforementioned defects when only PL data is considered.[20] Indeed, substantial efforts were made by some authors to overcome these difficulties and find convincing evidence for QC in systems of Si-NCs from optical data.[21,22] In stark contrast, STS provides information regarding the electronic density of states (DOS) and thus can directly measure the single-particle (not excitonic) band gap in a semiconductor (i.e., the conduction band to valence band separation). STS has been applied in studies of nanocrystalline Si assemblies; unfortunately, thus far, the individual NCs were not spatially separated and their surfaces were not well-defined.[18]

In this paper, we present a systematic combined STS and optical investigation of surface-functionalized Si-NCs as a function of size for various capping ligands. Quantum confinement is clearly revealed by STS for all capping ligands studied. In contrast, it is observed in the PL spectra only for Si-NCs functionalized with dodecene or trioctylphosphine-oxide (TOPO) but not for nitrogen-containing species, NH_4Br and allylamine. In addition, the tunneling spectra show shifts of the band-edges toward either positive or negative energy values, depending on the surface-functionalizing ligand and are akin to the effect of p-type and n-type doping, respectively.

The Si-NCs were prepared following the procedure described in ref 23. Briefly, solid hydrogen silsesquioxane (HSQ) was heated to 1100 °C in a slightly reducing atmosphere (5% H_2/95% Ar) for one hour. Upon cooling to room temperature, the resulting amber solid was ground into a fine brown powder. Subsequently, this Si-NC/SiO_2 composite was either treated further by heating in argon atmosphere to facilitate particle growth and size focusing[24] (followed again by grinding), or used directly in the next step. Hydride-terminated Si-NCs were liberated from the Si-NC/SiO_2 powder by HF etching then were transferred into toluene and immediately functionalized. Four types of ligands were used for surface functionalization: dodecene, TOPO, ammonium bromide (NH_4Br), and allylamine (see Supporting Information text and Supporting Information Figures S1, S2 for synthesis, functionalization, and characterization details). Functionalized Si-NCs were then isolated/purified by standard antisolvent precipitation, centrifugation, and redispersion procedures. Panels (a) and (b) in Figure 1 show transmission electron microscopy (TEM) micrographs of the 3.1 nm average sized particles after functionalization, while panels (c) and (d) depict images of 5.1 and 8.3 nm (average diameters) functionalized particles, respectively. The corresponding size distributions of the NCs, additional TEM micrographs, and X-ray diffraction data are shown in Supporting Information Figures S3 and S4.

The PL spectra were usually obtained by irradiation of the NC toluene solution with the 441 nm line of a GaN laser (unless otherwise noted). Emitted photons were collected with a fiber optic connected to an Ocean Optics USB2000

dx.doi.org/10.1021/nl400570p | *Nano Lett.* XXXX, XXX, XXX−XXX

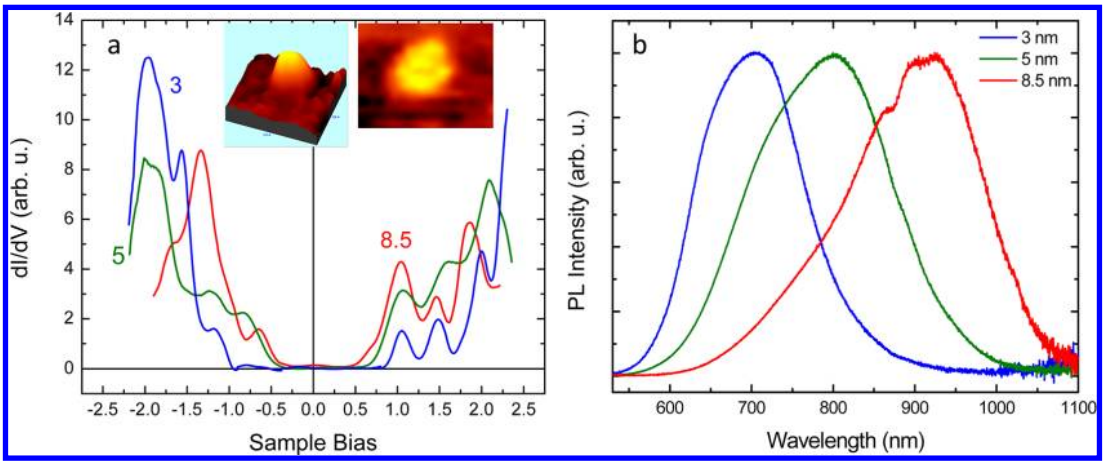

Figure 2. Size-dependent tunneling and PL spectra on dodecyl functionalized Si-NCs. (a) Three tunneling spectra measured on single isolated Si-NCs of different sizes, as indicated in the figure. The blue spectrum was measured on the 3 nm diameter NC presented in Figure 1c, the green curve was acquired on the NC shown in the right inset, and the red spectrum on the NC depicted by the left inset. (b) Three PL spectra measured on Si NC ensembles of average sizes around 3, 5, and 8.5 nm. Both the STS gaps and the PL maxima blueshift with reduction of NC size due to quantum confinement.

spectrometer. The spectrometer spectral response was normalized using a blackbody radiator.

For STM measurements, NCs were spin-cast from the toluene solution onto atomically flat flame-annealed Au substrates. All measurements were performed at room temperature using Pt–Ir tips. Tunneling current–voltage (I–V) characteristics were acquired after positioning the STM tip above individual NCs, realizing a double barrier tunnel junction (DBTJ) configuration[13] and momentarily disabling the feedback loop. In general, care was taken to retract the tip as far as possible from the NC, so the applied tip–substrate voltage would fall mainly on the tip–NC junction rather than on the NC–substrate junction whose properties (capacitance and tunneling resistance) are determined by the layer of organic capping ligands that cannot be modified during the STM measurement. This protocol minimizes the voltage division induced broadening effects, and thus the measured gaps correspond well to the real SC gaps.[13,15,17] The dI/dV–V tunneling spectra, proportional to the local tunneling DOS, were numerically derived from the measured I–V curves. We have acquired the topographic images and tunneling spectra (on the NCs) with bias and current set-values of $V_s \cong 1.2$–1.5 V and $I_s \cong 0.1$–0.3 nA. The first is to ensure tunneling above the band edge and the other was the lowest value that still allowed acquisition of smooth tunneling spectra. It should be noted that STM images of single NCs (presented as insets of all figures) do not lend themselves to accurate determination of the NC dimensions because of the convolution with the STM tip and the different DOS of the NC compared to its surroundings. Therefore, the NCs diameters used here are the average diameters determined from the TEM measurements, which were performed on ensembles from the same synthesis batch that was used for both the STS/STM and PL measurements. Importantly, relative NC sizes depicted by the STM images correlated well with average sizes determined from the TEM measurements.

Figure 2a presents three tunneling spectra acquired on single dodecyl-capped Si-NCs having three different diameters, ~3, 5, and 8.5 nm, all showing a clear gap in the DOS around zero bias (which is absent when measuring nearby the NCs, see Supporting Information Figure S5). The corresponding PL spectra, measured on ensembles from the same synthesis batch, are shown in Figure 2b. Both data sets clearly manifest trends attributable to QC. The PL maximum is blueshifted with decreasing NC diameter and, concomitantly, the gap in the DOS around zero bias increases (see also Figure 3 for cumulative data). With the STM settings used, where the voltage-division induced broadening is minimized, this zero-bias gap corresponds well to the energy gap of the NC.[13] We note, however, that the contribution of in-gap surface states to the DOS, which tend to reduce the apparent gap, cannot be ruled out. Since the STS measurements were performed at room temperature, the excited level structure is not well resolved in the tunneling spectra. Nevertheless, some general ligand-dependent spectral features, namely, supra band-edge peaks with spacing in the range calculated[25] for the addition energies, appear to persist in all spectra acquired on the same type of

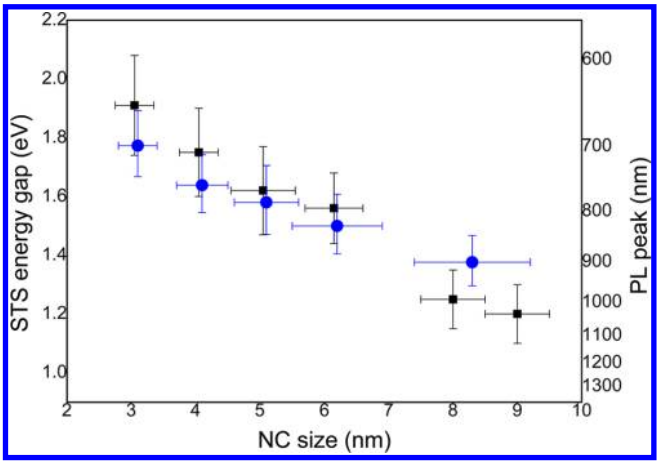

Figure 3. Energy gaps of dodecyl surface-terminated Si-NCs measured by STS (black squares) and PL maxima (blue dots) as a function of NC size. The vertical error bars represent the STS gap distribution and PL peak width respectively, and the horizontal bars depict the NC size distribution width. The PL and STS data points corresponding to the four smallest NCs were slightly shifted horizontally with respect to one another for clarity.

dx.doi.org/10.1021/nl400570p | Nano Lett. XXXX, XXX, XXX–XXX

ligand-capped NCs, although with different magnitudes, as also seen in Figure 4 below.

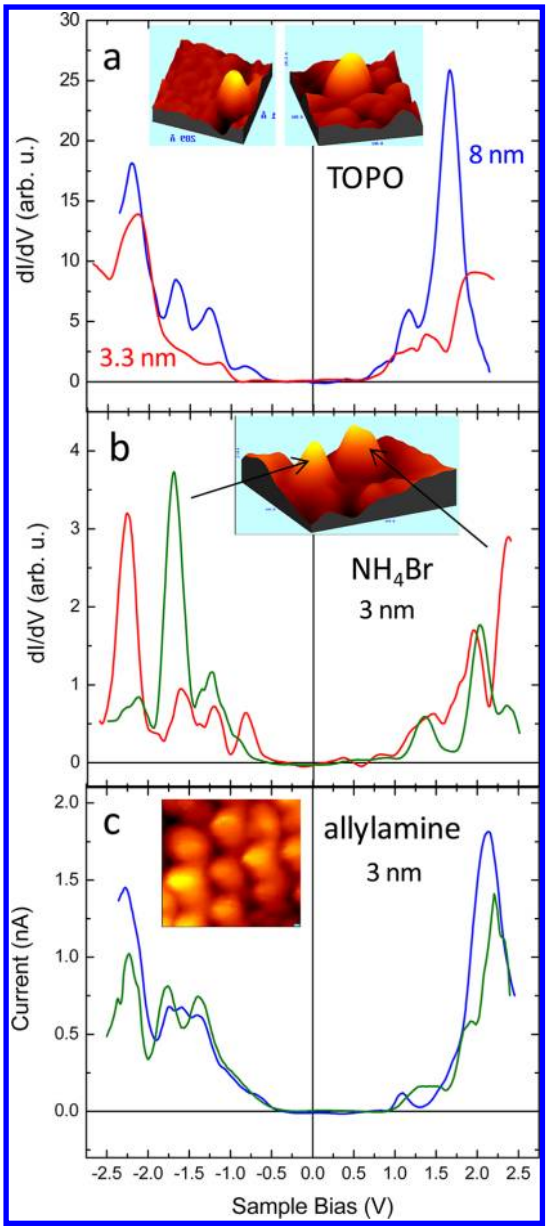

Figure 4. Effect of ligand-induced surface doping on Si-NCs. (a) Two tunneling spectra measured on TOPO functionalized Si-NCs of two sizes, one of 8 nm diameter (blue curve, right image) and the other 3.3 nm diameter (red curve, left image). (b) Same as (a), but for the two NH_4Br capped 3 nm NCs presented in the inset, as indicated by the arrows. (c) Two tunneling spectra measured on two different NCs within the cluster of allylamine functionalized NCs shown in the inset. It appears reaction with allylamine and NH_4Br induces p-type surface doping. The band-gaps measured on NCs within the arrays are smaller than those measured on isolated NCs.

The QC effect for dodecyl functionalized Si-NCs is clearly manifested in Figure 3, where the STS-extracted gap values are plotted along with the PL peak positions as a function of the Si NC diameter. The STS gaps were determined as follows: for each $dI/dV-V$ spectrum, the positions of the first peaks (or shoulders) at negative (valence band) and positive (conduction band) sides of the spectrum are found; this is denoted as the peak-to-peak gap. Next, the edge-to-edge gap is determined from the corresponding $I-V$ spectrum by noting the negative and positive voltages for which the current becomes detectable. The STS gap is then defined as the mean of the peak-to-peak and the edge-to-edge gap values. The standard deviations stemming from this calculation together with the distribution of gap values for different (more than twenty 3 nm diameter NCs, fourteen NCs of diameters in the range of 8–9 nms, and five to eight NCs of each of the other sizes) NCs constitute the vertical error bars for the STS gaps data (black squares). The error bars corresponding to the PL peaks relate to the full width at half-maximum (fwhm) of the PL spectra.

As shown by Figure 3, the energy gaps and PL maxima shift to higher energy with decreasing NC size, consistent with the QC effect. As expected, the STS gaps are larger than the PL gaps for the smaller NCs. This arises from both, the aforementioned voltage-division effect, and, more basically, the optical gap incorporates the electron–hole Coulomb interaction that reduces its energy with respect to the STS measured gap.[13,25] The observations that for the larger NCs the PL peaks are positioned very close to, and even surpass the STS-derived gaps, is quite surprising. One possible explanation for the reduced apparent STS gaps is the emergence of in-gap band-edge surface states, the relative effect of which should be more significant for larger NCs, where the influence of QC is smaller. Additionally, the PL intensity may be biased toward the small NCs in a given distribution, skewing and shifting the peak toward higher energy. The effect of QC was also observed for TOPO-terminated Si-NCs, manifesting in both the tunneling and PL spectra, as demonstrated by Figures 4a and Supporting Information Figure S6, respectively. Finally, we note that the agreement of the PL energies with the STS measured energy-gaps suggests that our NCs are free of oxygen-related defect states. Such gap-states are known to serve as radiative recombination centers, thus yielding a pronounced PL redshift with respect to the gap.[20,22]

We now turn the present discussion to the possible surface doping effects induced by the surface-bonded ligands as demonstrated in Figure 4. A fundamental outcome of doping in bulk semiconductors is a shift of the Fermi level toward the conduction band for n-type doping and, conversely, toward the valence band for p-type doping. Remarkably, and quite surprisingly (for reasons that will be discussed below), a shift of the Fermi level toward the valence band, consistent with p-type doping, is clearly identified in the $dI/dV-V$ tunneling spectra measured on Si-NCs with NH_4Br- and allylamine-derived surface capping, presented in Figure 4b,c, respectively. This behavior is very robust and was found in all spectra acquired on these types of NCs. For example, the two spectra plotted in Figure 4b were acquired on the two different NCs shown in the inset, both depicting asymmetry, where the valence band-edge is closer to zero-bias compared to the conduction-band edge. Note, the band gap determined from the spectrum plotted in red is slightly smaller than that from the spectrum plotted in green; this is consistent with the former being measured on a somewhat larger NC. A similar shift was also observed for NCs located within two-dimensional arrays, as shown by the two tunneling spectra portrayed in Figure 4c, which were acquired on two different NCs in the cluster shown in the inset. We note in passing that the band-gaps measured on NCs within arrays were somewhat smaller, by typically 80–100 meV, compared to those found on isolated dots. However, this proximity-induced redshift effect is far less pronounced

dx.doi.org/10.1021/nl400570p | Nano Lett. XXXX, XXX, XXX–XXX

than that previously observed for InAs NCs,[14] where the corresponding band gap reductions, arising from the proximity to neighboring NCs, were in the range of 300−350 meV. The larger effect observed for InAs NCs may arise partly from the much smaller electron effective mass in InAs ($\sim 0.027m_0$) compared to that in Si ($0.33m_0$; "the density of states effective mass"). A typical tunneling spectrum measured on an isolated allylamine-capped Si-NC, 3 nm in diameter, is presented in Supporting Information Figure S7 along with spectra obtained from two 8 nm diameter counterparts. In addition to the quantum confinement effect, the data show that the level-shift (doping) effect holds also for the larger N-terminated NCs.

The above systematic p-type doping-like effect was not observed for Si-NCs functionalized with dodecyl or TOPO ligands. The spectra measured on 3 nm NCs presented in Figures 2a and 4a show, if at all, an opposite asymmetry for the smaller NCs, where the Fermi energy is slightly closer to the conduction band-edge. Such an effective (small) n-type like doping behavior was also found for 4 nm dodecyl-passivated NCs (see Supporting Information Figure S8). Interestingly, it appears from these last three figures that (at least for the dodecyl and TOPO capped NCs) the band gap widening with decreasing NC size takes place mainly via the blueshift of the valence band-edge, consequently making them appear more n-type like as their diameter reduces. Such a behavior is to be expected from hydride surface-passivation (by residual H atoms), akin to the well-documented corresponding effect of valence-band receding and the concomitant induced n-type character in amorphous Si−H alloys.[26] This effect is enhanced as the NC size reduces mainly due to the corresponding increase in steric interactions, diminishing the relative surface area covered by ligands that replace bonded hydride moieties. Such a behavior of asymmetric QC effect was not observed in previous STS measurements performed on colloidal II−VI and III−V semiconductor NCs by us[18] or other groups.[15,17] It should also be noted here that for the latter compound semiconductor NCs the "conventional" TOP/TOPO ligands are not expected to exhibit a large effect on the electronic properties of the NCs because their surface bonding through van der Waals interactions is comparatively weak, in contrast to the covalent Si−C linkage in Si-NCs studied here.

The level shifts induced by NC surface functionalization, described above, can be analyzed within the general framework developed in studies of adsorbate-induced band-bending on the surface of bulk semiconductors (and in particular Si).[27] Of course, this should be carried out with caution because the concept of a space charge region, typically extending over tens to hundreds of nanometers in bulk semiconductors, does not directly apply for particles of diameters smaller than 10 nm.[28] Nevertheless, it is reasonable that the two main factors affecting the band-bending at bulk semiconductor surfaces, the molecular dipole (and its direction with respect to the surface) and the charge transfer between the molecule and the semiconductor,[9,27] are relevant also for the present system. For NCs with NH_4Br-derived surface chemistry, one would intuitively expect n-type doping effects to arise from the interaction between a Si-NC and nitrogen atoms or amine groups. This intuition stems from many examples where nitrogen serves as an n-type dopant for bulk Si and thin films,[29,30] while amine groups exhibit electron donor characteristics.[31] Our measurements show just the opposite behavior, suggesting that a different bonding configuration, more complex than simple Si−N bonding, is involved in our case. A reasonable ligand-bonding configuration that explains the observed "p-doping" effect can be proposed when considering the protocol used to functionalize the NCs. A recent work[19] shows that upon exposure to air or water a Si−O−N species forms on the NC surface. These surface groups are usually viewed as being electron withdrawing,[31] thus giving rise to a p-doped NC. In the case of NCs exposed to allylamine, an even stronger p-type like doping effect can be expected, since in addition to the above charge transfer associated with the Si−O−N surface group, the molecule has a dipole moment directed outward from the NC surface, which should give rise to further upward shift of the Si-NC energy levels, akin to the reminiscent band-bending effect in semiconductor surfaces. Interestingly, the PL spectra measured on these N-terminated Si-NCs differed significantly from the spectra obtained from NCs functionalized with TOPO and dodecyl moieties. Most significantly, the PL peaks were positioned at energies around 2.9−2.95 eV, nearly independent of NC size (see Figure 5), and

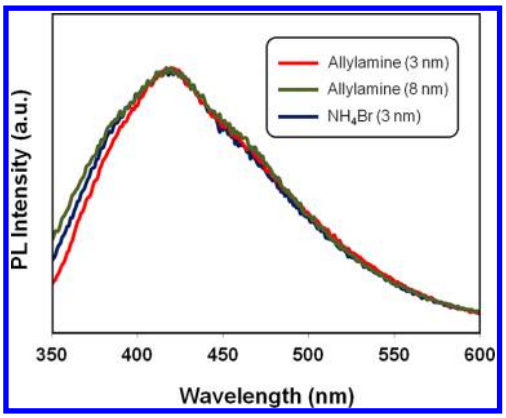

Figure 5. Photoluminescence spectra measured on Si-NCs 3 and 8 nm in diameter, functionalized with allylamine and 3 nm in diameter functionalized with NH_4Br. All spectra are anomalously shifted to the blue with respect to what is expected from band gap transitions in the corresponding NCs, and quantum confinement is not observed in contrast to the STS data in Supporting Information Figure S7. (Excitation λ = 325 nm).

therefore cannot be associated with the band gap. The origin and connection if at all exists between these anomalous PL spectra and the above p-type doping effect are not yet clear to us. We do note, however, that inconsistencies between optical spectroscopy data and band gap values were reported and discussed previously for various nanocrystalline Si systems.[32−34] Our present work thus demonstrates that tunneling spectroscopy is an essential tool for mapping the level structure of Si-NCs and in particular for determining the band gap.

The apparent slight n-type doping effect observed for the smallest (<4.1 nm) dodecyl functionalized Si-NCs is somewhat surprising, since the Si−C bond is slightly polarized toward the carbon atom (having higher electronegativity). However, the hydrogen atoms near the Si−C bond may change this trend (considering possible overlap between the Si orbitals and the C−H bonds). In addition, the aforementioned effect of gap widening due mainly to the blueshift of the valence band-edge may also contribute to the n-type like behavior in particular for the smaller NCs, as discussed above. The dipole moment of 1-dodecene is rather weak (~0.35 D) and is therefore not expected to affect much the level structure.

dx.doi.org/10.1021/nl400570p | Nano Lett. XXXX, XXX, XXX−XXX

In summary, tunneling spectroscopy measurements on single freestanding Si-NCs are reported here for the first time. The tunneling spectra manifest the quantum confinement effect via the increase of the single electron band gap with NC size reduction, and the measured band-gaps did not depend much on the surface functionalizing groups. A p-type doping-like effect, manifested by a shift of the band-edge toward lower energies, is found to take place upon surface functionalization with allylamine and NH_4Br, whereas a small opposite effect is observed for the smallest dodecyl-capped NCs. These behaviors may be attributed to the combined effects of the electrical dipole of the ligands and charge transfer between them and the NC. The QC effect manifested itself in the PL data only for dodecyl- and TOPO-terminated NCs, whereas anomalous PL spectra, which could not be accounted for by the NC level structure, were observed for the two N-terminated Si-NCs that exhibited p-type doping. STS is demonstrated here to be an essential method for the determination of the electronic level structure of Si-NCs. Control of the electrical properties with NC size and surface functionalization is an important step in the quest for implementing Si-NCs in optoelectronic and solar-cell devices.

■ ASSOCIATED CONTENT

Ⓢ Supporting Information

Reagents and materials, NC synthesis and functionalization, characterization and instrumentation, and additional figures as referenced in the text. This material is available free of charge via the Internet at http://pubs.acs.org.

■ AUTHOR INFORMATION

Corresponding Author

*E-mail: (O.M.) milode@mail.huji.ac.il; (J.G.C.V.) jveinot@ualberta.ca.

Notes

The authors declare no competing financial interest.

■ ACKNOWLEDGMENTS

We are thankful to Yehonadav Bekenstein for fruitful discussions and assistance in sample preparation. O.M and I.B acknowledge support from the Israel Science Foundation, the Harry de Jur Chair in Applied Science (O.M.) and the Enrique Berman Chair in Solar Energy Research (I.B.). The Veinot group acknowledges continued generous funding from the Natural Sciences and Engineering Research Council of Canada (NSERC), Canada Foundation for Innovation (CFI), Alberta Science and Research Investment Program (ASRIP). M.D. also recognizes support from the NSERC CGSD program and the Killiam Foundation.

■ ABBREVIATIONS

STS, scanning tunneling spectroscopy; Si-NCs, Si nanocrystals; PL photoluminescence; STM, scanning tunneling microscopy; QC, quantum confinement; DOS, density of states

■ REFERENCES

(1) Cole, J. R.; Mirin, N. A.; Knight, M. W.; Goodrich, G. P.; Halas, N. J. *J. Phys. Chem. C* **2009**, *113*, 12090−12094.
(2) Malko, A. V.; Mikhailovsky, A. A.; Petruska, M. A.; Hollingsworth, J. A.; Htoon, H.; Bawendi, M. G.; Klimov, V. I. *Appl. Phys. Lett.* **2002**, *81*, 1303.
(3) Medvedev, V.; Kazes, M.; Kan, S.; Banin, U.; Talmon, Y.; Tessler, N. *Synth. Met.* **2003**, *137*, 1047−1048.
(4) Kazes, M.; Lewis, D. Y.; Banin, U. *Adv. Funct. Mater.* **2004**, *14*, 957−962.
(5) Gur, I.; Fromer, N. A.; Geier, M. L.; Alivisatos, A. P. *Science (New York, N.Y.)* **2005**, *310*, 462−5.
(6) Bang, J. H.; Kamat, P. V *ACS Nano* **2009**, *3*, 1467−76.
(7) Li, L.; Daou, T. J.; Texier, I.; Kim Chi, T. T.; Liem, N. Q.; Reiss, P. *Chem. Mater.* **2009**, *21*, 2422−2429.
(8) Schipper, M. L.; Iyer, G.; Koh, A. L.; Cheng, Z.; Ebenstein, Y.; Aharoni, A.; Keren, S.; Bentolila, L. A.; Li, J.; Rao, J.; Chen, X.; Banin, U.; Wu, A. M.; Sinclair, R.; Weiss, S.; Gambhir, S. S. *Small* **2009**, *5*, 126−34.
(9) Soreni-Harari, M.; Yaacobi-Gross, N.; Steiner, D.; Aharoni, A.; Banin, U.; Millo, O.; Tessler, N. *Nano Lett.* **2008**, *8*, 678−84.
(10) Mocatta, D.; Cohen, G.; Schattner, J.; Millo, O.; Rabani, E.; Banin, U. *Science* **2011**, *332*, 77−81.
(11) Wills, A. W.; Kang, M. S.; Wentz, K. M.; Hayes, S. E.; Sahu, A.; Gladfelter, W. L.; Norris, D. J. *J. Mater. Chem.* **2012**, *22*, 6335.
(12) Ding, Z.; Quinn, B. M.; Haram, S. K.; Pell, L. E.; Korgel, B. a; Bard, A. J. *Science (New York, N.Y.)* **2002**, *296*, 1293−7.
(13) Banin, U.; Millo, O. *Annu. Rev. Phys. Chem.* **2003**, *54*, 465−92.
(14) Steiner, D.; Aharoni, A.; Banin, U.; Millo, O. *Nano Lett.* **2006**, *6*, 2201−2205.
(15) Bakkers, E. P. A. M.; Hens, Z.; Zunger, A.; Franceschetti, A.; Kouwenhoven, L. P.; Gurevich, L.; Vanmaekelbergh, D. *Nano Lett.* **2001**, *1*, 551−556.
(16) Liljeroth, P.; Overgaag, K.; Urbieta, A.; Grandidier, B.; Hickey, S.; Vanmaekelbergh, D. *Phys. Rev. Lett.* **2006**, *97*, 096803.
(17) Bakkers, E. P. A. M.; Vanmaekelbergh, D. *Phys. Rev. B* **2000**, *62*, R7743−R7746.
(18) Banin, U.; Cao, Y. W.; Katz, D.; Millo, O. *Nature* **1999**, *400*, 542−544.
(19) Dasog, M.; Yang, Z.; Regli, S.; Atkins, T. M.; Faramus, A.; Singh, M. P.; Muthuswamy, E.; Kauzlarich, S. M.; Tilley, R. D.; Veinot, J. G. C. *ACS Nano* **2013**, *7*, 2676−2685.
(20) Wolkin, M.; Jorne, J.; Fauchet, P.; Allan, G.; Delerue, C. *Phys. Rev. Lett.* **1999**, *82*, 197−200.
(21) Godefroo, S.; Hayne, M.; Jivanescu, M.; Stesmans, A.; Zacharias, M.; Lebedev, O. I.; Van Tendeloo, G.; Moshchalkov, V. V *Nat. Nanotechnol.* **2008**, *3*, 174−8.
(22) Alonso, M. I.; Marcus, I. C.; Garriga, M.; Goñi, A. R.; Jedrzejewski, J.; Balberg, I. *Phys. Rev. B* **2010**, *82*, 045302.
(23) Hessel, C. M.; Henderson, E. J.; Veinot, J. G. C. *Chem. Mater.* **2006**, *18*, 6139−6146.
(24) Yang, Z.; Dobbie, A. R.; Cui, K.; Veinot, J. G. C. *J. Am. Chem. Soc.* **2012**, *134*, 13958−61.
(25) Franceschetti, A.; Zunger, A. *Phys. Rev. B* **2000**, *62*, 2614−2623.
(26) Allan, D. C.; Joannopoulos, J. D. In *The Physics of Hydrogenated Amorphous Silicon II*; Joannopoulos, J. D., Lucovsky, G., Eds.; Springer: New York, 1983; pp (56) 5.
(27) Vasudevan, S.; Kapur, N.; He, T.; Neurock, M.; Tour, J. M.; Ghosh, A. W. *J. Appl. Phys.* **2009**, *105*, 093703.
(28) Balberg, I. *J. Appl. Phys.* **2011**, *110*, 061301.
(29) Pavlov, P. V.; Zorin, E. I.; Tetelbaum, D. I.; Khokhlov, A. F. *Phys. Status Solidi A* **1976**, *35*, 11−36.
(30) Temple-Boyer, P.; Jalabert, L.; Couderc, E.; Scheid, E.; Fadel, P.; Rousset, B. *Thin Solid Films* **2002**, *414*, 13−17.
(31) He, T.; Corley, D. A.; Lu, M.; Di Spigna, N. H.; He, J.; Nackashi, D. P.; Franzon, P. D.; Tour, J. M. *J. Am. Chem. Soc.* **2009**, *131*, 10023−30.
(32) Zou, J.; Baldwin, R. K.; Pettigrew, K. A.; Kauzlarich, S. M. *Nano Lett.* **2004**, *4*, 1181−1186.
(33) Shiohara, A.; Hanada, S.; Prabakar, S.; Fujioka, K.; Lim, T. H.; Yamamoto, K.; Northcote, P. T.; Tilley, R. D. *J. Am. Chem. Soc.* **2010**, *132*, 248−53.
(34) Kůsová, K.; Cibulka, O.; Dohnalová, K.; Pelant, I.; Valenta, J.; Fucíková, A.; Zídek, K.; Lang, J.; Englich, J.; Matejka, P.; Stepánek, P.; Bakardjieva, S. *ACS Nano* **2010**, *4*, 4495−504.